



Dipartimento di Meccanica e  
Tecnologie Industriali  
Università degli Studi di Firenze  
Italy



Dipartimento di Meccanica  
Politecnico di Torino - Italy



Belgium  
Abdelling PMA

in cooperation with



Union College - NY, USA



Society for Experimental  
Mechanics - CT, USA

# PROCEEDINGS OF THE FLORENCE MODAL ANALYSIS CONFERENCE

held under the auspices of the  
Consiglio Nazionale delle Ricerche

September 10-11-12, 1991

Palazzo degli Affari, Piazza Adua, 1 - Florence, Italy

# THEORETICAL - NUMERICAL MODAL ANALYSIS OF A PORTABLE GRINDER DISK

Angelo Farina<sup>†</sup>, Rinaldo Garziera<sup>†</sup>, Edzeario Prati<sup>‡</sup>

<sup>†</sup> Researcher at University of Parma, Industrial Engineering Department, Italy

<sup>‡</sup> Full prof. at University of Parma, Industrial Engineering Department, Italy

## Abstract

This work presents the analytical solution for the vibrations of a portable grinder disk, its elastic parameters evaluation by comparing experimental data [1] with calculated frequencies and, eventually, a numerical solution for vibrations under operating conditions which impose a very quick rotation to the disk. These results are worked out for two kinds of disks: normal disks and high internal damping disks, the latter having been recently introduced with the aim of noise reduction. A comparison between calculated data and experimental data obtained in [1] shows a good accordance between experimental apparatus and theoretical model.

## Nomenclature

$R_i$	Disk internal radius.
$R_e$	Disk external radius.
$h$	Disk thickness.
$w(x,y,t)$	Disk displacement
$E$	Young module.
$\kappa$	Poisson's ratio.
$\mu$	mass density per unit surface.
$\omega$	frequency.
$J()$	Bessel function of first kind.
$Y()$	Bessel function of second kind.
$I()$	Modified Bessel function of first kind.
$K()$	Modified Bessel function of second kind.
$p$	Radial load.
$q$	Tangential load.

## 1. Introduction

The increasing interest in acoustic pollution drives technicians and engineers to get concerned with new

methods for reducing industrial machinery acoustic emission in factories. Since acoustic emission is generally connected with the vibrations of some machine component, many of today researches are devoted to vibration control.

This article is related to the modal analysis and elastic parameters estimation of two classes of grinder disks: damped and non damped.

Since a grinder emits almost all of its noise through the vibration of its disk, the passive control with appropriate internal damping of these vibrations seems the most efficient way to reduce noise, increasing comfort for the operator. One of the techniques employed to make "damped disks" is to inclose into the abrasive agglomerate constituting the disk a sort of rubber layer which performs, through its hysteresis, a high internal damping action.

A full and very comprehensive experimental comparison between damped and non damped disks has been done by the same authors in [1] taking into account acoustic emission and experimental modal testing. In spite of its completeness, the experimental work [1] needs support by a theoretical-numerical approach in an interdependent way:

1) The comparison between experimental and calculated frequencies permits the determination of elastic parameters; these parameters, Poisson's ratio  $\kappa$  and Young Module  $E$ , are important for a characterization of the tested material, and their knowledge constitutes the basis for numerical investigations.

2) The numerical determination of normal modes can take account of centrifugal forces due to the disk rotation present while disk is operating; using these numerical

results we can validate the experimental tests and go beyond them estimating also frequencies not found in laboratory.

For these reasons, the present note is basically composed of three parts: the solution of free vibrations for a disk clamped on an inner circumference and free on the external boundary; the parameters estimation by comparing experimental and theoretical frequencies; a finite element modal analysis that takes into account disk rotation and graphically shows the first modes.

## 2. Theoretical modes evaluation

In this section the solution for the free vibrations of a circular plate clamped on its inner circumference  $R_i$  and free at  $R_e$  are worked out. Fig.1 shows the disk and the boundary constraints. We consider the plate lying in the  $xy$  plane with the deflection  $w(x,y,t)$  taking place along the  $z$  direction. We assume that the deflection is small compared to the plate thickness  $h$ , that no tangential action is present on the surface of the disk and we neglect the rotatory inertia forces due to bending. The displacement equation of motion for the free vibration is (see for instance [2])

$$\frac{Eh^3}{12(1-\kappa^2)} \nabla^2(\nabla^2 w) + \mu \frac{\partial^2 w}{\partial t^2} = 0 \quad (1)$$

where  $E$  denotes Young's module,  $\mu$  is the mass density per unit surface and  $\kappa$  is the Poisson's ratio.

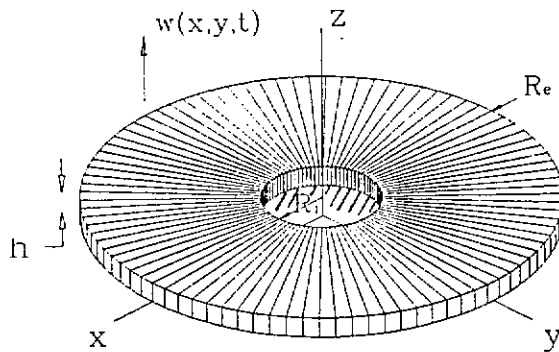


Figure.1. The disk

Since our boundaries are circular it is convenient to express the deflection  $w$  in cylindrical coordinates  $w(r,\vartheta,t)$ . In cylindrical coordinates the Laplace

operator reads

$$\nabla^2 = \frac{\partial^2}{\partial r^2} + \frac{1}{r} \frac{\partial}{\partial r} + \frac{1}{r^2} \frac{\partial^2}{\partial \vartheta^2} \quad (2)$$

With the separation of variables

$$w(r,\vartheta,t) = u(r,\vartheta)Y(t) \quad (3)$$

equation (1) splits in two

$$\frac{Eh^3}{12(1-\kappa^2)} \nabla^4 u - \mu \omega^2 u = 0 \quad (4)$$

$$\frac{d^2 Y}{dt^2} + \omega^2 Y = 0 \quad (5)$$

From eq.(4) taking (2) into account we obtain

$$\frac{\partial^2 u}{\partial r^2} + \frac{1}{r} \frac{\partial u}{\partial r} + \frac{1}{r^2} \frac{\partial^2 u}{\partial \vartheta^2} = \pm \gamma^2 u \quad (6)$$

in which  $\gamma^4 = \frac{12(1-\kappa^2)\mu\omega^2}{Eh^3}$

We apply again the separation of variables

$$u(r,\vartheta) = \phi(r)\xi(\vartheta) \quad (7)$$

eventually obtaining

$$r^2 \left[ \frac{d^2 \phi}{dr^2} + \frac{1}{r} \frac{d\phi}{dr} \right] \frac{1}{\phi} \pm \gamma^2 = n^2 \quad (8)$$

$$\frac{1}{\xi} \frac{d^2 \xi}{d\vartheta^2} = -n^2 \quad (9)$$

So the general solution of eq.(7) may be expressed as the product of two sets of functions satisfying eq. (8) and (9)

$$u = [a_n J_n(\gamma r) + b_n I_n(\gamma r) + c_n Y_n(\gamma r) + d_n K_n(\gamma r)] \cos(n\vartheta + \delta) \quad (10)$$

The first term of the product gives the radial shape of the disk, and contains Bessel functions of the first kind  $J(z)$  and of the second kind  $Y(z)$  plus Modified Bessel functions  $I(z)=J(iz)$  and  $K(z)=Y(iz)$ . The second term shows how diametrical nodes depend on  $n$ .

Remembering eq (3) and (5) we can express the vibration time dependency

$$w = u(r,\vartheta) \cos(\omega t + \psi) \quad (11)$$

A first boundary condition states the congruence of displacements along circumferences

$$u(r,\vartheta) = u(r,\vartheta + 2\pi) \quad (12)$$

from this equation and eq.(10) it immediately follows

that  $n$  must be an integer, that is: only Bessel functions of integer order have to be considered.

For the clamped circumference the deflection and the slope of deflection must be zero

$$u(r, \vartheta) = 0 \quad \text{for } r = R_1 \quad (13)$$

$$\frac{\partial u}{\partial r} = 0 \quad \text{for } r = R_1 \quad (14)$$

For the free edge the bending moment and the shearing force must be zero

$$\frac{1}{\kappa} \frac{\partial^2 u}{\partial r^2} + \frac{1}{r} \frac{\partial u}{\partial r} + \frac{1}{r^2} \frac{\partial^2 u}{\partial \vartheta^2} = 0 \quad \text{for } r = R_e \quad (15)$$

$$\frac{\partial}{\partial r} \left( \frac{\partial^2 u}{\partial r^2} + \frac{1}{r} \frac{\partial u}{\partial r} + \frac{1}{r^2} \frac{\partial^2 u}{\partial \vartheta^2} \right) + \frac{1-\kappa}{r^2} \frac{\partial^2}{\partial \vartheta^2} \left( \frac{\partial u}{\partial r} - \frac{u}{r} \right) = 0 \quad \text{for } r = R_e$$

Applying these conditions to eq.(10) we find at each  $n$  an homogeneous system of four equations with  $\mathbf{a} = \{a_n, b_n, c_n, d_n\}^T$  unknown.

$$Z_n \mathbf{a}_n = 0 \quad (17)$$

The coefficients of these four equations may be set in a 4x4 matrix, say  $Z_n$ , which must have determinant equal to zero in order to obtain non trivial solution for  $\mathbf{a}$ .

In full detail the elements of  $Z_n$  matrix are

$$Z_n = \begin{vmatrix} \zeta_{11} & \zeta_{12} & \zeta_{13} & \zeta_{14} \\ \zeta_{21} & \zeta_{22} & \zeta_{23} & \zeta_{24} \\ \zeta_{31} & \zeta_{32} & \zeta_{33} & \zeta_{34} \\ \zeta_{41} & \zeta_{42} & \zeta_{43} & \zeta_{44} \end{vmatrix}$$

$$\zeta_{11} = J_n \quad \zeta_{12} = I_n$$

$$\zeta_{13} = Y_n \quad \zeta_{14} = K_n$$

$$\zeta_{21} = \frac{n}{b} J_n - \gamma J_{n+1} \quad \zeta_{22} = \frac{n}{b} I_n + \gamma I_{n+1}$$

$$\zeta_{23} = \frac{n}{b} Y_n - \gamma Y_{n+1} \quad \zeta_{24} = \frac{n}{b} K_n - \gamma K_{n+1}$$

with all the Bessel functions calculated in  $\gamma R_1$

$$\zeta_{31} = \frac{n^2 \eta}{R_e} J_n - (n^2 \eta \gamma + \gamma^3) \left[ \frac{n}{\gamma R_e} J_n - J_{n+1} \right]$$

$$\zeta_{32} = \frac{n^2 \eta}{R_e} I_n - (n^2 \eta \gamma - \gamma^3) \left[ \frac{n}{\gamma R_e} I_n + I_{n+1} \right]$$

$$\zeta_{33} = \frac{n^2 \eta}{R_e} Y_n - (n^2 \eta \gamma + \gamma^3) \left[ \frac{n}{\gamma R_e} Y_n - Y_{n+1} \right]$$

$$\zeta_{34} = \frac{n^2 \eta}{R_e} K_n - (n^2 \eta \gamma - \gamma^3) \left[ \frac{n}{\gamma R_e} K_n - K_{n+1} \right]$$

$$\zeta_{41} = -\gamma R_e^3 \eta \left[ \frac{n}{\gamma R_e} J_n - J_{n+1} \right] + R_e^2 (n^2 \eta - \gamma^2) J_n$$

$$\zeta_{42} = -\gamma R_e^3 \eta \left[ \frac{n}{\gamma R_e} I_n + I_{n+1} \right] + R_e^2 (n^2 \eta + \gamma^2) I_n$$

$$\zeta_{43} = -\gamma R_e^3 \eta \left[ \frac{n}{\gamma R_e} Y_n - Y_{n+1} \right] + R_e^2 (n^2 \eta - \gamma^2) Y_n$$

$$\zeta_{44} = -\gamma R_e^3 \eta \left[ \frac{n}{\gamma R_e} K_n - K_{n+1} \right] + R_e^2 (n^2 \eta + \gamma^2) K_n$$

with all Bessel functions calculated in  $\gamma R_e$  and  $\eta = \frac{1-\kappa}{R_e^2}$ .

Note that care has to be taken in performing the second order derivatives  $\frac{\partial^2 u}{\partial r^2}$ . These derivatives have been worked out using eq.(6) which allows us to compute second order derivatives evaluating only first order derivatives of  $u$  with respect to  $r$  avoiding too expensive calculations; the sign for the right term of eq.(6) is minus for Bessel functions  $J$  and  $Y$  and plus for Modified Bessel functions  $I$  and  $K$  (see also [5]).

The determinant of matrix  $Z_n$  depends on  $R_1$ ,  $R_e$ ,  $\gamma$  and  $\kappa$ , while it does not depend on  $E$ . At any integer number  $n$ , which gives the number of diametrical nodes, we find infinite values of  $\gamma$  say  $\gamma_{n,m}$  satisfying equation  $\det(Z_n) = 0$ ,  $m$  giving the number of circumference nodes. Finally we can find the natural frequencies  $\omega_{n,m}$  from the definition of  $\gamma$ .

It can also be noted that  $\det(Z_n)$  does depend just on the two products  $\gamma R_1$ ,  $\gamma R_e$  and on the two parameters  $n$  and  $\kappa$  (it can be verified multiplying by  $R_1$  the second row of  $Z_n$  and by  $R_e^3$  the third row), so we may find for example solutions of  $\det(Z_n) = 0$  in term of  $\gamma_{n,m} R_e$  given the ratio  $R_1/R_e$ , the Poisson's ratio  $\kappa$ , and  $n$ .

Zeros of  $\det(Z_n)$  can be found whit a simple bisecting routine since  $\det(Z_n)$  is a smooth and well behaving function.

### 3. Experimental and theoretical data comparison versus parameters estimation

Since the value of  $\det(Z_n)$  depends on Poisson's ratio  $\kappa$ , which is unknown, a straightforward solution for eigenvalues is impossible.

While the value of  $\omega_{n,m}$  vary with the square root of  $E$ ,

the ratio between two frequencies, say for example  $\nu = \omega_{3,2}^2 / \omega_{5,4}^2$ , does not depend on Young's module. So, in principle, we could calculate  $\kappa$  trying to approach the ratio between any two experimental frequencies with the ratio between the two correspondent calculated frequencies. Nevertheless after a look at matrix  $Z_n$  it is easy to see that

$$\lim_{n \rightarrow \infty} \frac{\partial \gamma}{\partial \kappa} = 0 \quad (18)$$

and numerical investigations prove that already for  $n = 3$ ,  $\gamma_{n,m}$  is almost independent from  $\kappa$ . For this reason it seems convenient to consider the ratio

$$\nu = \frac{\gamma_{0,0}}{\gamma_{3,0}} = \nu(\kappa) \quad (19)$$

in which the numerator presents a good sensitivity on  $\kappa$  variations, and the denominator which can be considered constant for  $\kappa$  variations is related to a well evaluated experimental mode.

Starting from a trial value of  $\kappa$  in matrix  $Z_n$ , we can receive an approximate estimation of  $\nu$  and of the rate  $\frac{d\nu}{d\kappa}$  then we can calculate a better value of  $\nu$  using the Newton-Rapson formula

$$\kappa_{i+1} = \kappa_i - \nu(\kappa_i) \left. \frac{d\kappa}{d\nu} \right|_{\kappa_i} \quad (20)$$

This method gives sufficient precision after a very small number of iterations.

Table I shows the characteristics of two disks, normal and with high internal damping (the last one is called "silentium" after its commercial name), that come out applying the above outlined methods on the experimental data reported in [1] as well as in table IV and V.

Table I. Properties of standard and silentium disks

NON DAMPED	SILENTIUM
$\omega_{0,0} = 4618 \text{ rad/s}$	$\omega_{0,0} = 3990 \text{ rad/s}$
$\omega_{3,0} = 10870 \text{ rad/s}$	$\omega_{3,0} = 8922 \text{ rad/s}$
$\rho = 2560 \text{ kg/m}^3$	$\rho = 2560 \text{ kg/m}^3$
$\kappa = 0.19$	$\kappa = 0.26$
$E = 1.88e10 \text{ N/m}^2$	$E = 1.31e10 \text{ N/m}^2$

The interpretation of these values must take into account the nature of the disk material which is not

homogeneous. The "damped" disk is made of an abrasive agglomerate plus a rubber net lying in a "sandwich-like" manner in the middle of the disk. This kind of structure may recall layered materials for which special and quite complicated theories have been developed (see for instance [4]). In spite of this, it seemed appropriate and sufficient, at the present, to consider an homogeneous disk; the elastic properties reported in table I should be thought as belonging to this homogeneous model.

Table II reports the calculated frequencies for "non damped" disk while table III contains frequencies of "silentium" disk. These values have been obtained for the elastic properties shown in table I.

Table II. Modal frequencies (Hz) of "non damped" disk.

$m \setminus n$	0	1	2	3	4	5
0	735	721	954	1731	2933	4463
1	4716	5001	5902	7491	9715	12578
2	13788	1412	15175	17018	19710	23229

Table III. Modal frequencies (Hz) of "silentium" disk

$m \setminus n$	0	1	2	3	4	5
0	635	615	787	1422	2419	3693
1	4039	4273	5019	6347	8247	10631
2	11756	12038	12918	14467	16738	19713

Table IV and V reports the experimental data obtained testing respectively "non damped" and "silentium" disk; these tests are fully reported in [1].

Table IV. First experimental frequencies (Hz) of "non damped" disk

$m \setminus n$	0	1	2	3	4	5
0	735	505	915	1730	2950	4425

table V. First experimental frequencies (Hz) of "silentium" disk

$m \setminus n$	0	1	2	3	4	5
0	635	440	815	1420	2395	3610

Comparing tables II to table IV and III to V, we note a good accordance between experimental and theoretical data: only  $\omega_{1,0}$  does not match properly for either "silentium" and "non damped" disk. This frequency corresponds to the "hat-brim" mode reported in fig.4. This mode and the subsequent one, the "saddle-like" shown in fig.5, are very influenced by constraint geometry (i.e.  $R_1$  value). Probably the gripping apparatus of the disk, which has been fully described in [1] and which is the same used on grinders, did not guarantee a perfectly circular fixed joint of radius  $R_1$ .

#### 4. Numerical solution with centrifugal force

In order to find modes and frequencies of the disk in operating condition, i.e. while spinning at 8500 rpm, we must take centrifugal forces into account.

In presence of a radial load  $p$  and of a tangential load  $q$ , eq.1 becomes

$$\frac{Eh^3}{12(1-\kappa^2)} \nabla^4 w + \mu \frac{\partial^2 w}{\partial t^2} - \frac{h}{r} \frac{\partial}{\partial r} (p r \frac{\partial w}{\partial r}) - \frac{h}{r^2} q \frac{\partial^2 w}{\partial \theta^2} = 0 \quad (21)$$

which can be integrated only numerically (for example by the Ritz method).

We decide now to follow another way of solution: with the previous determined elastic properties, a numerical analysis is now possible with a finite element model.

In fig.2 the finite element mesh of the disk is shown.

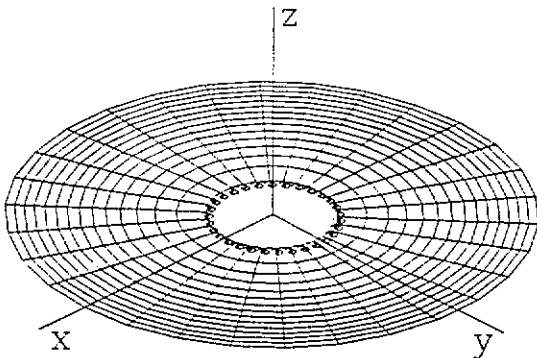


Figure 2. Finite element mesh.

The model for the finite element analysis (F.E.A.), is constituted of 420 "plate elements", (30 sectors by 14 tracks) having almost equal area to avoid orthotropic flaws in the solution. All the degrees of freedom are frozen for the nodes belonging to the inner circumference of radius  $R_1$ . The centrifugal forces acting on each element have been calculated for 8500 rpm and applied to the inner nodes of the elements themselves. These inertia forces vary from about 20 N on the inner elements to 70 N on the outer ones.

From this finite element model we obtain the common flexional modes mixed with the so called "membrane modes" which do not involve any disk bending. These non bending modes do not produce any sound so they are scarcely interesting and they are not reported.

Figs.3 to 10 show the first 10 modes and frequencies.

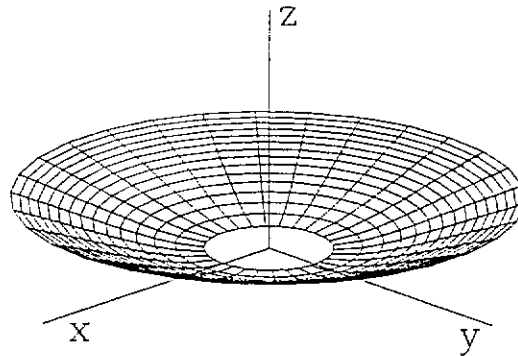


Figure.3. "Bowl-like" mode; non damped disk 750 Hz, silentium disk 649 Hz.

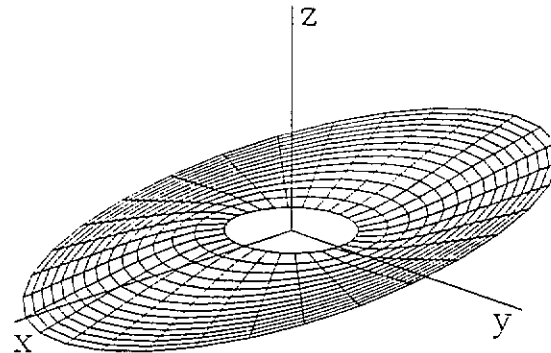


Figure.4. "Hat-brim" mode; non damped disk 741 Hz, silentium disk 635 Hz.

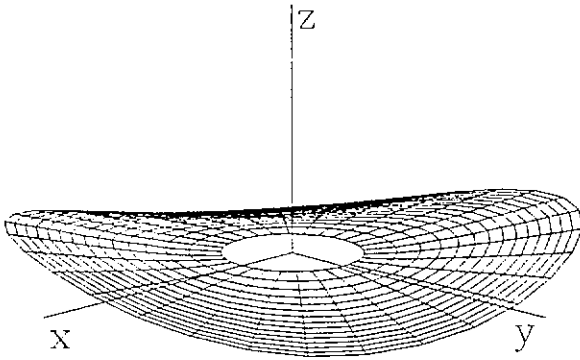


Figure.5 "Saddle-like" mode; non damped disk 983 Hz,  
silientium disk 919 Hz

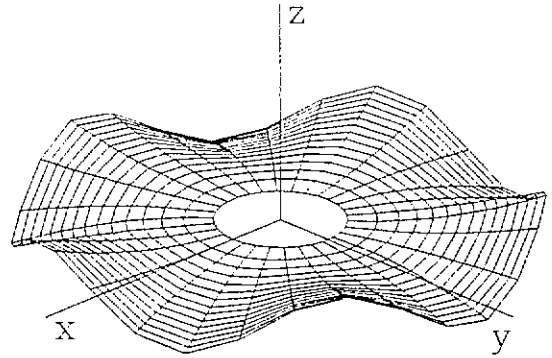


Figure.8.  $n=5, m=0$ ; non damped disk 4504 Hz,  
silientium disk 3735 Hz

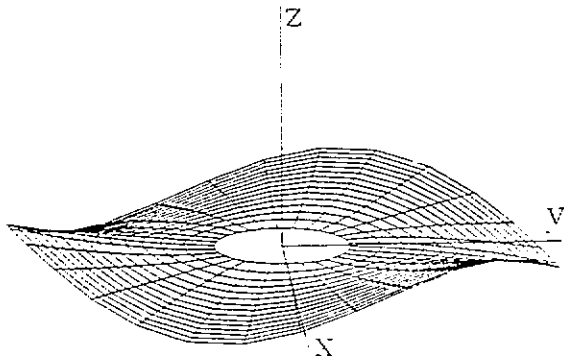


Figure.6.  $n=3, m=0$ ; non damped disk 1754 Hz,  
silientium disk 1451 Hz

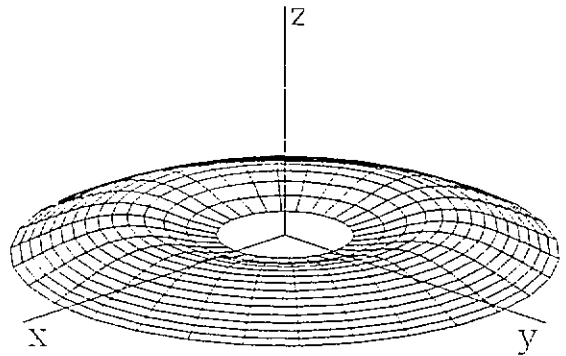


Figure.9.  $n=0, m=1$ ; non damped disk 4761 Hz,  
silientium disk 4082 Hz.

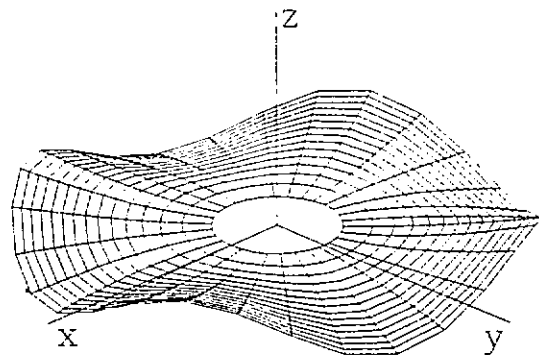


Figure.7.  $n=4, m=0$ ; non damped disk 2962 Hz,  
silientium disk 2449 Hz

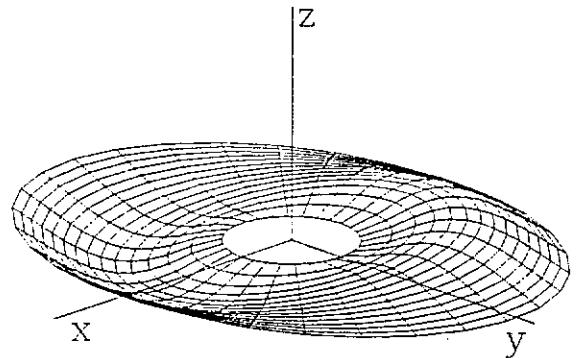


Figure.10.  $n=1, m=1$ ; non damped disk 5048 Hz,  
silientium disk 4319 Hz.

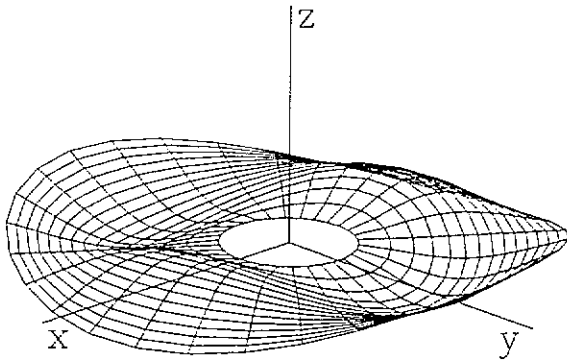


Figure.11.  $n=2, m=1$ ; non damped disk 5954 Hz,  
silentium disk 5083 Hz.

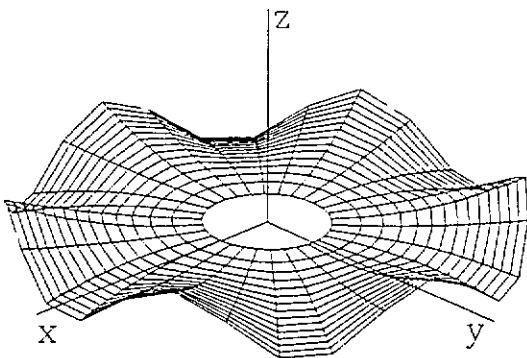


Figure.12.  $n=6, m=0$ ; non damped disk 6378 Hz,  
silentium disk 5301 Hz.

For the first five modes the frequencies obtained from F.E.A. - when compared to those reported in tables II and III - are 2% higher for non damped disk and 3% higher for "silentium" disk. This is only due to the centrifugal forces since an F.E.A. without these inertia forces gives frequencies that very closely approach tables II and III (errors less than  $2^0/00$ ).

##### 5. Model's adequacy discussion and conclusions

The theoretical model, for whom an analytical solution of equation (1) has been worked out, gives results in a good accordance with the experimental data.

The analytical solution together with the experimental data let us find the elastic properties of the disks. Silentium disks are less stiff and have a higher Poisson's ratio than standard disks: differences are due to the rubber layer presence.

Theoretical and experimental frequencies do not match only for the "hat-brim" mode; this could probably be avoided by changing the design of the gripping device in the experimental apparatus, but rising the risk of loosing contact with real tools.

From the F.E. analysis it has resulted that taking into account centrifugal forces in predicting the vibration frequencies results in very small differences. On the other hand, calculating frequencies by using eq.(17) and forcing  $\det(Z_n)$  to zero takes the "runs" a thousand times shorter than by F.E.A.

Nevertheless, F.E.A. provided in a straightforward manner the clarifying figures 2 to 12 representing the normal modes; these figures could also be drawn on the basis of the theoretical solution, but it would have been a complicated and time-wasting experience.

In future developments of this research some theoretical considerations about the forcing action and the nature of damping will be done.

##### Acknowledgements

The authors wish to thank Dr. Giorgio Borrè and Dr. Roberto Garziera for having been running SUPERSAP many and many times and for their suggestions in F.E.A.

Work partially supported by CNR 90.00872.CT07 entitled "Effetto dei giochi sulla precisione di movimenti di meccanismi".

##### Bibliography

- [1] Farina A., Garziera R., Prati E., "Experimental modal analysis of a portable grinder disk", *Florence Modal Analysis Conference*, September 1991.
- [2] Rayleigh J.W.S., 1945, *The theory of sound* vol.1 Dover.
- [3] Inman D.J., 1989, *Vibration with control measurement and stability*, New York Prentice-Hall.
- [4] Torvik, P.J., 1980, "The analysis and Design of Constrained Layer Damping Treatments." *Damping Applications for Vibration Control*. ASME AMD-38:85-112.
- [5] Gatteschi L. 1973, *Funzioni speciali*, Torino UTET.